

A Highly Efficient Diversity-based Input Selection for DNN Improvement Using VLMs

Amin Abbasishahkoo, Mahboubeh Dadkhah, Lionel Briand, *Fellow, IEEE*

Abstract—Maintaining or improving the performance of Deep Neural Networks (DNNs) through fine-tuning requires labeling newly collected inputs, a process that is often costly and time-consuming. To alleviate this problem, input selection approaches have been developed in recent years to identify small, yet highly informative subsets for labeling. Diversity-based selection is one of the most effective approaches for this purpose. However, they are often computationally intensive and lack scalability for large input sets, limiting their practical applicability. To address this challenge, we introduce Concept-Based Diversity (CBD), a highly efficient metric for image inputs that leverages Vision-Language Models (VLM). Our results show that CBD exhibits a strong correlation with Geometric Diversity (GD), an established diversity metric, while requiring only a fraction of its computation time. This makes CBD an efficient and scalable alternative for guiding repetitive, extensive input selection scenarios. Building on this finding, we propose a hybrid input selection approach that combines CBD with Margin, a simple uncertainty metric. We conduct a comprehensive evaluation across a diverse set of DNN models, input sets, selection budgets, and five most effective state-of-the-art selection baselines. The results demonstrate that the CBD-based selection consistently outperforms all baselines at guiding input selection to improve the DNN model. Particularly, the CBD-based selection achieves an average accuracy improvement percentage of 38% across various budget sizes for ImageNet, which corresponds to a 6.7 percentage points increase relative to the second-best performing baselines. Furthermore, the CBD-based selection approach remains highly efficient, requiring selection times close to those of simple uncertainty-based methods such as Margin, even on larger input sets like ImageNet. These results confirm not only the effectiveness and computational advantage of the CBD-based approach, particularly compared to hybrid baselines, but also its scalability in repetitive and extensive input selection scenarios.

Index Terms—Deep Neural Network, Input Selection, Diversity Score, Vision Language Model.

I. INTRODUCTION

Deep Neural Networks (DNNs) have been used in a wide range of application domains, including computer vision, health, and particularly software engineering [1], [2], [3]. Similar to traditional software, DNNs require continuous updates to maintain and improve their performance, particularly as new inputs become available. However, manually labeling all newly collected inputs, whether for testing or fine-tuning, is often impractical due to the substantial time and effort required. Input selection addresses this challenge by identifying and

Amin Abbasishahkoo is with the School of EECS, University of Ottawa, Ottawa, ON K1N 6N5, Canada (e-mail: aabba038@uottawa.ca).

Mahboubeh Dadkhah is with the School of EECS, University of Ottawa, Ottawa, ON K1N 6N5, Canada (e-mail: mdadkhah@uottawa.ca).

Lionel Briand is with the School of EECS, University of Ottawa, Ottawa, ON K1N 6N5, Canada, and also with the Research Ireland Lero centre for software, University of Limerick, Ireland (e-mail: l briand@uottawa.ca).

Manuscript received March 1, 2025.

labeling only a small, yet highly informative subset of the candidate inputs. Subsequently, fine-tuning the DNN on this carefully selected subset may enable the model to achieve performance comparable to training on the full set of new inputs while significantly reducing labeling costs. In recent years, several input selection methods have been proposed, mostly by the software engineering community [4], aiming to improve DNN model performance while reducing fine-tuning costs. Diversity-based selection approaches are widely used and highly effective for this purpose; however, they tend to be computationally expensive, especially when dealing with large unlabeled input sets in practice. To overcome this limitation, we introduce a highly efficient Concept-Based Diversity (CBD) metric for measuring the diversity of image input sets, leveraging Vision-Language Models (VLM). Building on this metric, we further present a hybrid input selection approach that leverages both diversity and uncertainty to guide fine-tuning of vision DNNs (DNNs that process images as inputs), providing not only effective but also efficient model improvement.

VLMs are deep learning models that learn joint visual-textual representations through training on massive collections of image-text pairs. The proposed CBD metric leverages CLIP (Contrastive Language-Image Pretraining) [5], a prominent VLM that comprises an image encoder and a text encoder that jointly map their respective inputs to a shared multimodal embedding space. This shared space enables us to calculate the similarity between an image embedding and a set of text embeddings, and extract the most representative concepts for each image. Subsequently, the CBD score for an image input set is calculated based on the diversity of the concepts extracted from images in that set. To alleviate the overhead of running CLIP for each image input, we adopt a recent technique (described in the subsequent section) to map an image representation in the DNN model to its corresponding representation in CLIP’s shared embedding space, enabling highly efficient CBD calculation.

Diversity metrics have been successfully used for input selection both in traditional software and in DNN models [6], [7]. A recent comprehensive study on diversity metrics for image input sets, showed that Geometric Diversity (GD) is the most effective metric in capturing the actual diversity of an image input set [7]. Despite its demonstrated effectiveness, measuring diversity efficiently remains a major concern, particularly for metrics that require pairwise distance calculations over large input sets, which can become computationally expensive, and for input selection methods that require measuring diversity across a large number of candidate subsets.

In contrast, the proposed CBD metric effectively and ef-

ficiently measures the diversity of an input set based on the natural-language concepts that represent images in the set. The efficiency of the CBD score calculation, enabled by leveraging VLMs, is particularly important in the context of input selection, as in such scenarios, a large number of candidate input subsets are often examined until the final input subset is selected. Compared to well-established input diversity metrics such as GD, CBD provides a comparable diversity measurement effectiveness, with significantly less computation time. Similar to GD, the CBD score is independent of the DNN model’s characteristics; thus, it can reliably measure input diversity even when the model has low accuracy.

In addition to diversity metrics, uncertainty metrics, including Margin [4], can also be leveraged for selection. While these metrics are highly efficient and effective at detecting DNN failures, they are less effective in guiding model improvement. This is because they often prioritize inputs near the decision boundary in the input space, where many inputs share similar characteristics, leading to redundancy among the selected inputs. In contrast, diversity metrics help identify input sets with more diverse, non-redundant inputs. However, diversity-based approaches might select inputs that are likely to be correctly predicted by the model and thus not contribute to model improvement.

To address the limitations of using either uncertainty or diversity alone, hybrid selection methods have been proposed that combine both of these metrics [8], [6]. Although Hybrid selection approaches are generally more effective at guiding model improvement, they are often computationally expensive because they require calculating the diversity through pairwise distances in the high-dimensional feature space of many candidate input subsets before final selection. In this paper, we propose a hybrid input selection approach based on our CBD metric that not only consistently outperforms state-of-the-art (SOTA) baselines in guiding DNN model improvement but also remains highly efficient.

We empirically evaluated our proposed CBD metric in measuring the actual diversity of input sets. Our results on two subject models and input sets, across various subset sizes (1%, 3%, 5%, 7%, and 10% of each original test set), demonstrate that our proposed CBD score has a strong correlation with the GD score, an established diversity metric, indicating its high potential to guide DNN model improvement. Furthermore, CBD is highly efficient, with calculation time approximately 2.5 to 36 times faster than GD while delivering comparable diversity measurement performance.

Moreover, we performed a comprehensive study to evaluate our CBD-based input selection and compared it with five SOTA baselines. Given the study’s extensive scope and high computational cost, we limited our comparison to the most effective and computationally feasible selection approaches. Conducting our experiments took approximately 32 days (excluding interruptions). This substantial computational cost stems from several factors: the large number of baselines, subjects, and selection budgets considered; the time-intensive process of fine-tuning DNN models using selected input subsets; and the need to repeat the fine-tuning process five times for each combination of baseline, subject, and selection

budget to account for the inherent stochasticity of DNN fine-tuning.

The results demonstrate that our CBD-based selection approach consistently outperforms baselines in improving the DNN model across all subjects and selection budgets through fine-tuning. We also compared the time required to select subsets with the same selection budgets for the CBD-based approach and all the investigated baselines. Notably, the CBD-based selection approach remains highly efficient, requiring computation time comparable to that of simple uncertainty-based methods such as Margin. Moreover, compared to other hybrid and diversity-based selection baselines, the CBD-based approach reduces the selection time by more than three orders of magnitude, making it not only practical but also highly scalable, even for larger input sets such as ImageNet [9].

The key contributions of this paper are as follows:

- An efficient metric for measuring the diversity of image input sets using VLMs, named CBD. Our empirical evaluation shows that CBD is not only effective at measuring the actual diversity of an input set but is also highly efficient. Consequently, CBD is a practical and scalable metric for repetitive and extensive input selection from larger input sets such as ImageNet.
- A CBD-based input selection approach capable of effectively guiding DNN model improvement while featuring a competitive efficiency. The proposed approach combines CBD and uncertainty scores to select a small yet diverse and informative subset for effectively fine-tuning the DNN model.
- An extensive evaluation that took approximately 32 days to complete, comparing the proposed CBD-based selection with five SOTA baselines across two subject DNN models and input sets, including the large ImageNet. The results indicate that the CBD-based approach consistently outperforms all baselines, achieving significantly greater improvements in model accuracy when fine-tuning with subsets selected under the same selection budget.

The remainder of this paper is organized as follows: Section II provides background, including a brief overview of the input selection baselines used in our experiments and a summary of VLMs and concept extraction from images. Section III introduces the proposed CBD metric and presents the CBD-based approach for input selection. Section IV describes the experimental design used to evaluate the CBD metric and the CBD-based selection approach. Section V reports and discusses the results for each research question. Section VI reviews related work, and Section VII concludes the paper.

II. BACKGROUND

This section provides an overview of the main categories of SOTA input selection approaches, used as baselines in our evaluations. Additionally, since we introduce a new concept-based method for calculating the diversity of an input set that leverages VLMs, we also review VLMs and discuss how they can be utilized to automatically extract concepts from image inputs.

A. Input Selection for DNN improvement

This section reviews related work on input selection approaches for enhancing DNN models, which we consider baselines in our evaluations. To make our experiments feasible in terms of computational resources, we intentionally exclude certain existing input selection approaches based on their reported effectiveness or computational cost. Specifically, we exclude approaches that have been comprehensively studied and evaluated in prior work and that are outperformed by some baselines included in our experiments.

For instance, Adaptive Test Selection (ATS) [10] introduced by Gao *et al.* has consistently been outperformed by more recent baselines [6], [4]. ATS iteratively selects inputs based on the dissimilarity between each remaining input and the currently selected subset, making it one of the most computationally intensive selection approaches [4]. Similarly, Surprise Adequacy (SA) metrics, proposed by Kim *et al.* [11], and Neuron coverage (NC) metrics [12], [13] are among the white-box methods that have been excluded due to their limited effectiveness. SA metrics measure how surprising an input is relative to the DNN model's training input set, while NC metrics consider the neuron activation ranges. Both ATS and coverage-based metrics have also been consistently outperformed by more recent selection approaches in terms of improving DNN performance [10], [4], [6], [8].

1) **Uncertainty metrics:** The primary objective of selection approaches based on uncertainty metrics is to identify and select inputs for which the DNN model is less confident in its prediction [14]. Consequently, they tend to select inputs that are close to the decision boundary. Since these methods focus on uncertainty rather than diversity, the selected inputs might not cover a wide or representative region of the DNN's input space. However, some of these methods have proven effective not only for detecting DNN faults but also for guiding model improvement [4], [15], [14], [16]. Therefore, in this section, we review uncertainty-based methods that have been shown to effectively guide model improvement.

Uncertainty metrics measure the DNN model's confidence in predicting an input, either by analyzing the model's predicted probability distribution [4] for the given input or by leveraging information from the input's nearest neighbors within the input set. DeepGini [14], Margin [4], and Vanilla-Softmax [15] are widely-known metrics that rely solely on the model's predicted probability for the given input. However, DeepGini and Vanilla-Softmax have been outperformed by other baselines [6], [16], [8] in terms of improving the accuracy of DNN models. Therefore, we exclude them from our experiments. The Margin score quantifies a model's confidence in distinguishing its top two predicted classes for an input x , defined as the difference between the highest (p_m) and second-highest (p_n) predicted probabilities: $\text{Margin}(x) = p_m(x) - p_n(x)$.

Recent research has investigated using the neighbors' information of a given input to estimate the model's uncertainty in predicting it [16], [17]. One of the most effective methods in this category is DATIS (Distance-Aware Test Input Selection), proposed by Li *et al.* [16], which has been shown

to outperform prior input selection techniques in both fault detection and model performance improvement [18], [16]. Unlike uncertainty metrics that rely solely on predicted probabilities, DATIS estimates uncertainty based on the ground-truth labels of the input's nearest neighbors within the DNN model's labeled training set. First, it calculates the support of the training inputs for the DNN's prediction for a given input x . This support is computed by summing the exponentials of the distances between the given input and its closest training neighbors. Specifically, the support of the training inputs for predicting an input x as part of class $c \in Y$ based on its k -nearest neighbors in the training set is calculated as follows:

$$p_c^*(x) = \frac{\sum_{t \in \text{Train}_k(x)} \exp(-\|z(x) - z(t)\|_2^2 / \tau) \mathbb{I}(y(t) = c)}{\sum_{t \in \text{Train}_k(x)} \exp(-\|z(x) - z(t)\|_2^2 / \tau)} \quad (1)$$

where $\text{Train}_k(x)$ is the list of x 's k -nearest neighbors in the training set, τ is a scaling parameter controlling the influence of distances in the latent space, and $z(x)$ and $z(t)$ are the latent feature representation of the given input x and its nearest neighbor t , respectively. $\mathbb{I}(\cdot)$ represents an indicator function that equals 1 if the predicted label of the training input $y(t)$ matches class c , and 0 otherwise. After calculating $p_c^*(x)$ for each class $c \in Y$, an estimation $p^*(x) = \{p_1^*, p_2^*, \dots, p_C^*\}$ for the input x is obtained. Then the DATIS uncertainty score for x is calculated as follows:

$$\text{DATIS}(x) = p_n^* / p_m^* \quad (2)$$

where m is the class predicted by the DNN model for input x , which may or may not correspond to the class with the highest support $p_c^*(x)$. $n = \arg \max_{c \in Y, c \neq m} p^*(x)$ denotes the most supported prediction distinct from the DNN predicted class m . Therefore, a higher value of $\text{DATIS}(x)$ indicates that the DNN's prediction for x is weakly supported by the training inputs.

2) **Diversity metrics:** Unlike uncertainty metrics, diversity metrics measure how well the inputs in an input set collectively cover different regions of the input or feature space. Aghababaeyan *et al.* [7] conducted a comprehensive study on black-box, model-agnostic diversity metrics for image inputs, including Normalized Compression Distance, Standard Deviation, and GD. These metrics measure diversity without requiring access to the model's internals. As they are independent of the DNN model itself, they can reliably measure the diversity of an input set even when the model's accuracy is low. Their results show that GD is the most effective metric for capturing the true diversity of an input set and, thus, for selecting inputs to test and improve DNN models [7]. They also demonstrate that GD shows a statistically significant correlation with fault detection in DNNs, outperforming other evaluated diversity metrics [7]. Building on this finding, they proposed DeepGD [6], a hybrid search-based approach that integrates GD with DeepGini for input selection. Another metric, introduced by Gao *et al.* [10], measures the dissimilarity between an input and a candidate set using the local fault patterns defined by clustering the inputs based on the model's output. Building on this metric, they proposed an adaptive

input selection method, ATS, aiming to select a diverse set of inputs that can effectively detect faults and improve the accuracy of the DNN model.

Despite their effectiveness, a major limitation of most diversity-based selection methods lies in their substantial computational cost. Specifically, methods that require calculating pairwise distances between inputs or measuring the dissimilarity between each input and a selected subset are among the most expensive and inefficient input selection methods [10], [7], [4]. Furthermore, this cost grows substantially with the size of the input set, thereby limiting the scalability of these methods in scenarios requiring extensive testing and making them even more impractical for larger input sets. For instance, Hu *et al.* [19] showed that deploying ATS incurs substantial computational overhead, particularly on larger input sets, where its execution time grows substantially compared to other already demanding approaches.

3) **Hybrid methods:** Hybrid input selection approaches aim to leverage the complementary strengths of multiple criteria to enhance effectiveness. In particular, several approaches combine uncertainty and diversity metrics [8], [6]. Approaches that rely solely on uncertainty metrics are generally efficient but tend to select inputs near the decision boundary, often leading to redundant inputs that have the same contribution to the DNN model’s improvement. In contrast, approaches that focus solely on diversity aim to select inputs that differ in the feature space, thereby reducing redundancy. However, they might select inputs that are likely to be correctly predicted by the DNN model and, therefore, are less effective for improving the model. By combining these two perspectives, hybrid approaches balance both aspects to select more effective and representative input subsets.

For instance, Aghababaeyan *et al.* developed DeepGD [6], an input selection approach that combines both GD and Deep-Gini metrics. To achieve this, their multi-objective search-based approach deploys Non-dominated Sorting Genetic Algorithm (NSGA-II). Their comprehensive evaluations demonstrate that DeepGD achieves superior performance not only in detecting a diverse range of faults but also in effectively guiding input selection to improve DNN performance. Even with small selection budgets, the input subsets selected by DeepGD consistently and significantly improve the model’s accuracy compared to uncertainty-based, coverage-based, and other diversity-based approaches such as ATS [10]. However, as discussed in the following sections, the limitation of DeepGD is its high computational overhead, making it computationally expensive in practice.

Wang *et al.* address the computational limitation of DeepGD by introducing SETS (Simple yet Effective Test Selection), a hybrid two-phase selection approach designed to minimize the number of costly diversity calculations. SETS proposes a light-weight, greedy algorithm that combines uncertainty and diversity for input selection. In the reduction phase, it filters out low-uncertainty inputs, retaining only those with a higher likelihood of detecting faults. The number of retained inputs is controlled by a user-defined parameter α , which determines the proportion of inputs preserved for selection. In the original implementation, α is set to retain three times the final selection

budget (i.e., $\alpha = 3 * b$), focusing only on the most uncertain inputs. Then, in the selection phase, the reduced candidate set is partitioned into equidistant sub-groups based on sorted uncertainty, ensuring even coverage across uncertainty levels. Rather than evaluating all candidates in each selection step, it selects only one input from each sub-group using a fitness function that combines uncertainty and normalized diversity gain. This reduces the total number of diversity evaluations from quadratic (in standard greedy selection) to linear in the number of candidate inputs, significantly reducing diversity computation cost.

While SETS achieves substantial efficiency gains by aggressively limiting the number of diversity calculations, this restriction has a noticeable impact on its effectiveness, as evidenced by our results discussed in the following sections. By filtering out a large portion of low-uncertainty inputs in the early reduction phase, SETS significantly lowers computational cost, particularly for large input sets. However, this early pruning can affect the quality of the final selected subset, especially for smaller values of α , as many potentially valuable inputs that could detect diverse faults or contribute to model improvement may be discarded prematurely. Moreover, in the selection phase, SETS further constrains diversity by selecting only one input from each sub-group, which may again exclude potential inputs, further limiting retraining effectiveness in certain settings.

Robust Test Selection (RTS) proposed by Sun *et al.* [8] is another hybrid input selection method that combines uncertainty with diversity for input prioritization. RTS divides unlabeled candidate inputs into three distinct sets: noise, suspicious, and successful (correctly classified) based on the model’s output probability distributions. Then it selects sequentially from these sets in a fixed priority order: first from suspicious, then from successful, and finally from noise inputs. To prioritize inputs in each set, RTS uses a novel probability-tier-matrix-based metric. As a result, RTS not only focuses on the diversity of the selected inputs, but it also avoids prioritizing inputs that are likely to be correctly predicted by the model. Their comprehensive evaluations demonstrate RTS’s superior effectiveness in both fault detection and model improvement compared to uncertainty-based, coverage-based, and surprise-based selection approaches [8].

B. Concept extraction from image inputs using VLMs

1) **Vision Language Models:** Recent advancements in artificial intelligence have led to the emergence of VLMs, a new category of models that learn joint representations from both visual and textual inputs. Unlike traditional vision models that rely on manually labeled input sets with fixed labels, VLMs are trained on massive collections of image-text pairs. This large-scale, multimodal training enables them to generalize across diverse tasks and domains and, more importantly, to represent and describe visual concepts in natural language.

CLIP [5], proposed by OpenAI, is one of the well-known VLMs and consists of two encoders that have been trained jointly: an image encoder (such as a ResNet or Vision Transformer) and a text encoder (a Transformer model). Each

encoder maps its input to a shared multimodal embedding space. Training is conducted using a contrastive learning objective on a dataset of 400 million image-text pairs extracted from the Internet. During the training phase, the model learns to maximize the similarity between matching image and text representations while minimizing the similarity between mismatched ones. Specifically, in each training batch of N (image, text) pairs, CLIP learns to predict which of the $N \times N$ possible pairings are correct, optimizing a symmetric cross-entropy loss over cosine similarity scores. This joint training enables the model to embed any image and its corresponding natural-language prompt (e.g., "a photo of a dog") into a single space, where similarity can be computed directly.

In inference, CLIP has been used to perform zero-shot classification by comparing an image's embedding with those of a set of text prompts containing all ground-truth labels of an input set (e.g., "a photo of a car", "a photo of a cat"), and selecting the one with the highest similarity score. Similarly, it can be used for extracting related concepts from image inputs. To achieve this, an image's embedding can be compared with those of a set of text prompts containing a diverse set of related concepts in the underlying input domain. Subsequently, concepts with the highest similarity can represent the image. For instance, consider a general input set containing images of different animals and a general knowledge base, such as ConceptNet [20]. As depicted in the lower part of Figure 1, for each concept, such as "standard poodle", we create a set of prompts containing that concept. For example, consider using the following prompt templates:

- "A photo of a" + concept
- "A drawing of a" + concept

For example, for the concept "standard poodle", two prompts are constructed: "A photo of a standard poodle" and "A drawing of a standard poodle". Then, each prompt is processed by CLIP's text encoder to obtain its corresponding embedding, and the average of these two embeddings is calculated to represent a single embedding for each concept [5], [21]. Similarly, we create two prompts for each concept in the knowledge base and average their embeddings to form a diverse set of concept embeddings. Given an image, it is processed by CLIP's image encoder to obtain its embedding, which is then compared against all concept embeddings. Consequently, the concepts whose corresponding embeddings achieve the highest similarity scores are selected as the ones representing that image.

2) *Knowledge bases for concept extraction*: To extract concepts from an input set of images, we require a knowledge base containing a diverse set of related concepts in the underlying application domain. A variety of general taxonomies and ontologies are available, including WordNet [22], ConceptNet [20], as well as more specialized domain-specific ontologies.

In addition to general-purpose knowledge bases, there are specific visual concept sets designed for vision-based tasks, such as the Visual Genome scene graph [23] and the Open Images dataset [24]. Visual Genome is a large-scale dataset with annotated scene graphs, representing visual concepts as

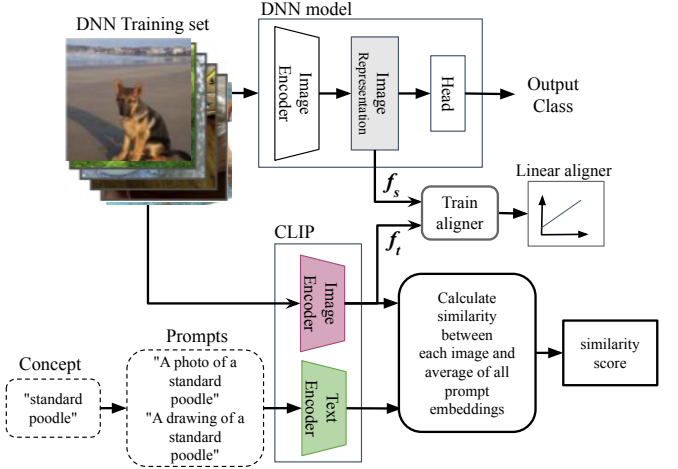


Fig. 1: Calculating similarity score between an image and a natural language concept using CLIP (lower part), and training a linear aligner between a DNN's internal representation and CLIP's shared embedding space (upper part).

objects, attributes, and relationships in images. This dataset defines more than 100,000 object categories and 40,000 attribute categories, along with spatial and functional relationships (e.g., on top of, holding, wearing). The resulting structure is a graph of visual entities, where nodes represent objects or attributes, and edges capture pairwise relationships. Unlike purely linguistic resources such as WordNet or ConceptNet, the Visual Genome ontology is grounded in visual semantics, making it highly relevant for vision-based tasks and for bridging the gap between image content and conceptual representation.

In our experiments, we consider two main criteria for selecting a knowledge base: 1) to contain visual concepts, i.e., concepts that represent entities or objects that can be observed in an image, and 2) to contain concepts corresponding to the application domain of our subject input sets. Since we performed our experiments on general image input sets such as ImageNet, as outlined in subsequent sections, we leverage the list of objects from the Visual Genome scene graph [23], which represents general visual concepts. It is important to note that while our proposed CBD metric is not limited to general domain applications, applying it to a domain-specific input set requires selecting an appropriate knowledge base that captures diverse domain concepts.

3) *DNN to VLM image representation alignment*: To extract related concepts from an input image using CLIP, each input image must be processed by CLIP's image encoder to obtain its corresponding embedding in the shared space. As a result, in an input selection scenario involving an extensive set of candidate inputs, CLIP must be executed once for each candidate input, leading to significant computational overhead. In particular, for hybrid input selection approaches that leverage both the DNN model's output for uncertainty calculation and CLIP's similarity scores for diversity calculation, eliminating the need for repeated CLIP executions can substantially improve efficiency.

Moayeri *et al.* [21] has shown that the representation of

an image in a model can be mapped to its representation in another model using a simple linear alignment. The task of mapping between a source vision encoder f_s to a target vision encoder f_t (i.e., $h : f_s(\mathcal{X}) \rightarrow f_t(\mathcal{X})$) can be learned by minimizing the mean squared error between the target encoder's embedding of an image and the source encoder's embedding after applying a trained linear transformation. In other words, this mapping is achieved by solving the following optimization problem:

$$W, b = \arg \min_{W, b} \frac{1}{|D_{\text{train}}|} \sum_{x \in D_{\text{train}}} \|W^T f_s(x) + b - f_t(x)\|_2^2.$$

where D_{train} represents the training set and a vision encoder is a model f that maps images $x \in \mathcal{X}$ to vectors $f(x) \in \mathbb{R}^d$. The mapping h is also restricted to the class of affine transformations, i.e.,

$$h_{W,b}(z) := W^T z + b.$$

They investigated widely used vision models, such as the ResNet series and CLIP [5], and reported that such mappings can be learned surprisingly well with just a single linear layer [21]. This finding suggests that, in input selection approaches where the representations of input images in the DNN model are already available, a linear aligner can be used to map those representations to CLIP's shared embedding space, as illustrated in the upper part of Figure 1. Consequently, CLIP's corresponding embeddings can be obtained without directly executing CLIP on every new input, thus substantially reducing computational cost and improving efficiency. In our input selection approach described in Section III, we build and use a linear aligner for each DNN model to efficiently extract concepts for each image, without running CLIP directly.

III. APPROACH

In this section, we first introduce our concept-based diversity (CBD) metric for image input sets, calculated by analyzing the concepts that represent the images in the set. To investigate its efficiency and effectiveness in guiding input selection to improve the DNN model, we present a hybrid selection approach leveraging CBD.

A. Concept-based diversity metric

The overall process of calculating the proposed CBD metric includes two main steps. The first, presented in Algorithm 1, is an initialization step and needs to be performed only once for each DNN and its corresponding training set. The second step, presented in Algorithm 2, calculates the diversity of a given unlabeled input set and can be applied multiple times to many input sets.

1) **Initialization step:** This initial step has two objectives: train a linear aligner to map the DNN model's image representation to its embedding in CLIP's embedding space, and construct a set of human-interpretable concepts that span the concept space on which the DNN model has been trained. To achieve the former, as described in Algorithm 1, each training image img_i is fed into both the DNN model and

Algorithm 1: Constructing RCS and training a linear aligner between a DNN and CLIP embedding spaces

Input:

N : the DNN model

$TrainSet$: the labeled training input set of N

$ImgEncoder_{CLIP}$: CLIP's image encoder

$TxtEncoder_{CLIP}$: CLIP's text encoder

KNB : Knowledge base

Output:

RCS : Representative Concept Set

$Aligner_N$: Trained linear aligner between N and CLIP spaces

```

1) Train a linear aligner between  $N$  and CLIP spaces
1 foreach image  $img_i$  in  $TrainSet$  do
2    $f_{s_i} \leftarrow GetDNNRepresentation(img_i);$ 
3    $f_{t_i} \leftarrow GetCLIPEmbedding(img_i);$ 
4    $Aligner_N \leftarrow TrainLinearAligner(f_s, f_t);$ 
2) Construct RCS
5  $ConceptList \leftarrow LoadConcepts(KNB);$ 
   Extract each concept's CLIP embedding
6 foreach concept  $cnp_j$  in  $ConceptList$  do
7    $PmtList \leftarrow CreatePrompts(cnp_i);$ 
8    $EmbList \leftarrow GetCLIPEmbedding(PmtList);$ 
9    $fe_j \leftarrow Average(EmbList);$ 
   Extract each image's top  $m$  concepts
10 foreach image embedding  $ft_i$  in  $ft$  do
11   foreach concept embedding  $fe_j$  in  $fe$  do
12      $SmtList \leftarrow Similarity(ft_i, fe_j);$ 
13    $topConcepts \leftarrow TopConcepts(SmtList, m);$ 
14    $A \leftarrow AddtoArchive(topConcepts);$ 
   Select unique concepts
15  $RCS \leftarrow RemoveDuplicates(A);$ 
   Save RCS concepts corresponding CLIP embeddings
16  $RCSemb \leftarrow SaveEmbeddings(fe, RCS);$ 
17 return  $RCSemb, Aligner_N$ 

```

CLIP to obtain the DNN's internal representation, and CLIP embeddings, denoted as f_{s_i} and f_{t_i} , respectively (lines 1-3). Using these paired embeddings for every training image, an accurate linear aligner can be built from the DNN representation space to the CLIP space (line 4). This aligner plays a crucial role in the efficiency of the CBD calculation, enabling fast, accurate concept extraction for unseen, unlabeled inputs in subsequent steps. By leveraging the DNN's representation of an input and mapping it to CLIP's embedding space using the aligner, concept extraction can be performed without directly invoking CLIP for every new input, significantly reducing computational cost. In Section IV-C, we report the accuracy of the aligners built in our experiments and investigate efficiency improvements achieved using the aligner compared to directly extracting the concepts with CLIP. The results show that an accurate aligner can be built for each DNN model, enabling efficient and accurate concept extraction.

In the initialization step, a set of highly related concepts,

called the Representative Concept Set (RCS), is also created from the images in the training set, collectively representing the semantic concept space on which the DNN model has been trained. While this process has traditionally required extensive manual effort to annotate images, the introduction of VLMs enables automatic concept extraction. To achieve this, we rely on existing knowledge bases that include concepts describing the underlying domain knowledge specific to each input set, as described in Section II-B2.

First, all concepts are retrieved from the selected knowledge base (line 5). Next, for each concept in the knowledge base, we create a set of natural language prompts and encode them using CLIP’s text encoder (lines 7 and 8). The most widely used prompt template for image inputs follows the pattern “A photo of [concept]”. However, specialized prompt templates can be adapted or extended depending on the input set and application domain to achieve more precise concept representations. The complete set of prompt templates used for each input set in our experiments is available in our replication package [25]. We adopt the process of using multiple prompt templates for each concept as proposed in the original paper [5] and widely adopted in subsequent works [21], to mitigate CLIP’s sensitivity to prompt phrasing and boost its performance. As a result of this process, we obtain multiple embeddings for each concept based on its associated prompts. Then, we calculate the average of these embedding vectors to achieve a single embedding for each concept [5], [21] (line 9).

Now that we have obtained the embeddings for all concepts fe , and the corresponding embeddings of the training images in CLIP’s shared embedding space ft , previously extracted during linear aligner training, we calculate the similarity score between each image and all concept embeddings (lines 10-12). We then select the top m most similar concepts for each image and add them to an archive list of all top concepts across the training set (lines 13 and 14). Finally, we remove duplicate concepts from the list, and a set of unique, highly related concepts constitutes the RCS of the input set (line 15). The embeddings of all RCS concepts in CLIP’s shared space are stored for the subsequent step of our approach, where they are utilized to calculate the diversity score of an input set (line 16). The goal of creating RCS is not only to obtain a set of concepts that represent the specific concept space of each input set, but also to improve CBD calculation efficiency by preventing similarity calculations between each new unlabeled image and unrelated concepts in the knowledge base. As a result, to extract concepts representing each unlabeled image in the input selection step, instead of investigating the image’s similarity to all concepts in the knowledge base, we only calculate its similarity to the concepts in RCS.

2) **CBD score calculation step:** In this step, we efficiently calculate the CBD score of a given unlabeled image input set using the RCS and the aligner constructed in the previous step, without running CLIP, as described in Algorithm 2. First, the embeddings of the concepts in the RCS obtained and stored during the initialization step are retrieved (line 1). Then, each image in the unlabeled input set is processed by the DNN model, its internal representation is extracted, and then mapped to CLIP’s shared embedding space, leveraging

Algorithm 2: CBD-score calculation for an unlabeled input subset TS

Input:

N : the DNN model

RCS : Representative Concept Set

$Aligner_N$: Trained linear aligner between N and CLIP spaces

TS : Unlabeled input set

Output:

CBD : CBD score of input set TS

Load RCS concepts corresponding CLIP embeddings

```

1  $RCSEmb \leftarrow LoadRCSEmbeddings(RCS);$ 
2 Map image embeddings with the trained linear aligner
3 foreach image  $I_i$  in  $TS$  do
4    $fs_i \leftarrow GetDNNRepresentation(I_i);$ 
5    $ft_i \leftarrow Map(Aligner_N, fs_i);$ 
6   Calculate similarity of an image to RCS concepts
7   foreach image  $ft_i$  in  $ft$  do
8     foreach concept  $fe_j$  in  $RCSEmb$  do
9        $SmtList \leftarrow Similarity(ft_i, fe_j);$ 
10       $topConcepts_i \leftarrow TopConcepts(SmtList, m);$ 
11      Calculate CBD
12      foreach concept  $con_c$  in  $topConcepts$  do
13         $fq(con_c) \leftarrow$  frequency of  $con_c$  across all concepts
14        in  $topConcepts$  in
15         $totalFreq \leftarrow \sum_{j=1}^k fq(con_j)$ 
16        foreach concept  $con_c$  in  $topConcepts$  do
17           $p_c \leftarrow \frac{fq(con_c)}{totalFreq}$ 
18         $CBD(TS) \leftarrow -\sum_{j=1}^k p_j \log_2(p_j)$ 
19      return  $CBD(TS)$ 

```

the linear aligner constructed in the previous step (lines 2-4). Subsequently, the similarity scores are computed between each mapped image embedding and all RCS concept embeddings (lines 5-7). Finally, for each image, the top m most similar concepts are selected to represent its semantic content (line 8), which serves as the basis for calculating the concept-based diversity score.

Figure 2 illustrates the efficient process we used to identify the most similar concepts from the RCS for each input image. As shown, each image is first processed by the DNN model to calculate the uncertainty score based on the model’s output probabilities, while its representation in the DNN’s internal space is extracted concurrently. The trained linear aligner then maps this representation into CLIP’s shared embedding space, eliminating the need to execute CLIP’s image encoder. Moreover, the embeddings of all RCS concepts in the CLIP embedding space are extracted and stored during the initialization phase (Algorithm 1) to be reused in this phase, thus avoiding repeated executions of CLIP’s text encoder. As a result, the computational overhead of concept extraction is limited to a forward pass through the linear aligner and similarity calculations between image and concept embeddings. We

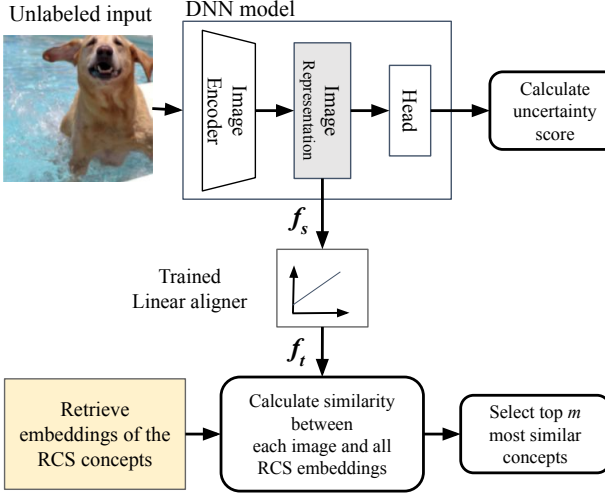


Fig. 2: The efficient process of finding highly similar concepts for each image using the RCS and the trained linear aligner.

further discuss the efficiency of the CBD score calculation, and we elaborate on this process in Section IV-C.

To calculate the diversity of an input set based on concepts extracted from its input images, we use the Shannon Entropy (lines 9-14). Let $TS = \{I_1, I_2, \dots, I_b\}$ denote the selected input set with size b , where each input image I_i is represented by a set of m most similar concepts $topConcepts(I_i) = \{Con_1, Con_2, \dots, Con_m\}$. While optimizing m enhances the ability of the CBD score to capture the true diversity of an input subset and thereby improves selection effectiveness, we set $m = 10$ in our experiments using a lightweight manual procedure. Specifically, for each input set, we sampled a representative subset of images and manually analyzed the concepts with the highest similarity scores. Based on this inspection, we identified a cutoff point beyond which the remaining concepts were weakly related to the input images and largely constituted noise. A comprehensive optimization of m would require extensive additional experiments, which is computationally infeasible given the already high cost of our current experiments. Therefore, we leave a more thorough investigation of this parameter as future work. In our experiments, as discussed in the following sections, we set $m = 10$. Let $fq(Con_c)$ denote the frequency of concept Con_c across the entire input set TS . The probability of observing a concept Con_c is then defined as:

$$p_c = \frac{fq(Con_c)}{\sum_{j=1}^k fq(Con_j)}$$

where k is the total number of distinct concepts observed in TS . Then, we calculate the CBD score of TS as the Shannon entropy of the input set's concept distribution as follows:

$$CBD(TS) = - \sum_{j=1}^k p_j \log_2(p_j)$$

Algorithm 3: CBD-based input selection approach

Input:

N : the DNN model
 $CandidateSet$: the unlabeled candidate set for input selection
 b : Selection budget

Output:

$Selected$: Selected input subset

```

1) Rank all inputs based on their uncertainty score
1 foreach input  $x_i$  in  $CandidateSet$  do
2    $U_i \leftarrow CalculateUncertainty(x_i);$ 
3  $Candidates \leftarrow SortDescend(CandidateSet, U);$ 
4) Select a diverse subset based on CBD score
5   Select an initial set of inputs
6    $Selected \leftarrow null;$ 
7    $b_{init} \leftarrow b/10;$ 
8    $j \leftarrow 0;$ 
9   while  $j \neq b_{init}$  do
10     $Concat(Selected, Candidates_j);$ 
11     $j \leftarrow j + 1;$ 
12
13 Continue selection with non-redundant inputs
14 while  $j \neq b$  do
15    $Temp \leftarrow Concat(Selected, Candidates_j);$ 
16   if  $CBDScore(Temp) > CBDScore(Selected)$ 
17     then
18        $Selected \leftarrow Temp;$ 
19    $j \leftarrow j + 1;$ 
20
21 return  $Selected$ 

```

which measures how uniformly the input set spans its related concepts. A higher entropy value reflects a more balanced distribution of concepts, indicating greater diversity.

B. CBD-based input selection

In this section, we combine our proposed CBD metric with simple uncertainty metrics to introduce a hybrid approach to input selection. Our goal is to develop a selection approach that is not only competitive with SOTA baselines in guiding DNN model improvement but also remains highly efficient. Evaluating this CBD-based input selection approach enables us to investigate both the effectiveness and scalability of the CBD metric in the context of input selection, where the diversity of a large number of candidate subsets must be computed repeatedly.

To combine the CBD score with the input uncertainty, the proposed CBD-based input selection approach, as described in Algorithm 3, consists of two main steps. First, all inputs are ranked in descending order of their uncertainty scores (lines 1-3) to prioritize selecting inputs for which the DNN model exhibits low confidence. These are the most informative inputs, and fine-tuning the model with them can effectively enhance its performance. However, many of these inputs are redundant and thus unable to contribute to model improvement. To address this, in the second step, the CBD score is employed

to detect and eliminate redundant inputs, ensuring the final selected subset remains diverse.

To achieve this, we start by selecting a small initial subset of the most uncertain inputs, corresponding to a fraction of the selection budget (lines 4–8). In our experiments, for a selection budget of size b , we initialize the subset with $0.1b$ inputs. We then traverse the remaining inputs in descending order of uncertainty and evaluate them one by one based on their ability to increase diversity of the currently selected subset (lines 9–13). Specifically, for each candidate input, we temporarily add it to the current subset and compute the resulting CBD score. If this temporary subset achieves a higher CBD score than the current one, the input is accepted, and the selected subset is updated. Otherwise, the input is discarded, and the next candidate in the ordered list is investigated. This process continues until a final subset of size b is selected.

By combining these two efficient and complementary criteria, the proposed CBD-based selection approach aims to select a subset that is both highly informative and diverse, enabling the fine-tuned model to achieve greater performance improvements within a constrained selection budget.

IV. EXPERIMENT DESIGN

A. Research Questions

We performed an extensive evaluation to answer our four key questions regarding both the effectiveness and efficiency of calculating the proposed CBD score, as well as the overall performance of the presented input selection approach, as follows:

RQ1: Does the proposed CBD metric effectively measure the diversity of an input subset? To answer this question, as in related studies on diversity metrics [7], we can perform a controlled experiment by creating a large number of input subsets with systematically increasing actual diversity. Then, for each subset, we compute the concept-based diversity and observe how it changes as the actual diversity increases [7]. In classification problems, a practical way to increase the actual diversity of a subset is to start by randomly selecting all inputs from a single output class, then incrementally increasing the number of covered classes by replacing some inputs with new ones sampled from different classes [7].

However, a more comprehensive method for evaluating our proposed CBD metric is to investigate whether it correlates with an established input diversity metric that, based on a comprehensive study, has already been shown to align with actual diversity and to significantly correlate with fault detection capability [7]. As discussed in Section II-A2, the GD score has been identified through extensive empirical studies as the most effective diversity metric for DNNs, reliably measuring actual input diversity and exhibiting a positive, statistically significant correlation with faults in DNNs [7]. Consequently, this analysis allows us to evaluate the effectiveness of the CBD metric for input selection and efficiently guiding DNN model improvement.

RQ2: Is the proposed CBD metric efficient?

To answer this question, we compare the cost of calculating the diversity of an input subset using the proposed metric

with that of the GD score [7], an established diversity metric for DNNs. As discussed in Section II-A2, diversity metrics are among the most computationally expensive and inefficient input selection methods. Notably, their computational cost increases rapidly with larger input sets, often exponentially, making them impractical. Consequently, to provide a comprehensive comparison of computational efficiency, we measure and compare the execution time required to compute each metric for input subsets corresponding to 1%, 3%, 5%, 7%, and 10% of the original test set, thus investigating the scalability and efficiency of each metric on larger input sets.

RQ3: Does the proposed CBD-based input selection approach guide DNN model improvement more effectively than baselines?

To answer this question, we investigate the effectiveness of our input selection approach in guiding DNN model improvement and compare it with the baseline selection methods described in Section II-A. For this purpose, we compare the accuracy improvements achieved through fine-tuning the DNN model with the input subset selected by the proposed approach and each baseline. We perform our evaluations across different selection budgets of 3%, 5%, 7%, 10%, 15%, and 20% of the original test set for each subject.

RQ4: Is the proposed CBD-based input selection approach efficient?

In this research question, we evaluate the efficiency of the proposed CBD-based selection approach by comparing its input selection time with that of the baselines. In particular, since diversity-based input selection methods are often among the most computationally expensive, our goal is to determine whether leveraging the proposed CBD metric can achieve not only high effectiveness in guiding input selection but also substantial improvements in computational efficiency.

B. Subjects

We conducted our experiments using a collection of well-known image input sets, including Cifar-10 [26], and ImageNet [9] that have been utilized in numerous empirical studies on DNN testing [27], [6], [28], [29], [30]. ImageNet is a widely recognized large-scale input set designed for visual object recognition research in the field of computer vision. It includes over 14 million labeled images across 1,000 object categories [9]. We leverage its most commonly used subset, ImageNet-1k, from the ILSVRC2012 competition, with a training set of 1,281,167 images and a validation set of 50,000 images for evaluation. Cifar-10 is another widely used input set that includes images from 10 classes (e.g., cats, dogs, airplanes, cars). Cifar-10 contains 32x32 cropped colored images, while images in the ImageNet input set are 224x224 pixels and feature higher resolution.

TABLE I: Information about the input sets and DNN models

input set	Model	Training set size	Test set size
Cifar-10	ResNet18	50,000	10,000
ImageNet	ResNet101	1,281,167	50,000

Using these input sets, we trained two DNN models using ResNet18 [31], and ResNet101 [31], as detailed in Table I. Note that, to avoid any selection bias, we reused the training and test sets defined in the original sources of these input sets [26], [9]. In our experiments, we use the training set to create an RCS and train a linear aligner for each input set and DNN model. We subsequently use the test sets for input selection, model fine-tuning, and evaluation, as described in the next section.

C. Linear aligner training

As described in Section III-A, in our proposed approach, we use a linear aligner to map the representation of the DNN model of an input to its representation in CLIP’s embedding space. While such an aligner is not part of this paper’s contribution, it is one of the components of the proposed approach and affects its results. Thus, in this section, we investigate the accuracy and the computational cost of the aligners we have built for each subject DNN model in our experiments. The detailed information on the trained aligners is presented in Table II. Initially, it is important to note that, as Moayeri *et al.* [21] have shown in their original paper for mapping the representation of an image in a source model to that of a target model using a simple linear alignment, the differences in the representation sizes of the two models significantly impacts the ability to train an accurate aligner. Specifically, when the source model’s representation size is smaller than the target model’s embedding size, building an accurate aligner becomes challenging, often resulting in reduced accuracy. Consequently, both the architecture of the subject DNN models in our experiments and the selected layer for their representation extraction affect the achievable accuracy of the trained aligner. However, the trained linear aligners achieved high accuracy, with R^2 values of 0.83 for Cifar-10 and ResNet18, and 0.72 for ImageNet and ResNet101. These values are comparable to the R^2 values reported by Moayeri *et al.* [21] for ImageNet and ResNet-based models. Moreover, our results presented in the next section indicate that this level of accuracy is sufficient to produce reliable CBD scores, demonstrating that the linear aligners perform well enough for highly effective CBD-based input selection and model improvement. We should note that to extract the representations, we used the outputs of the penultimate layer of the DNN models, as this layer captures the most informative and semantically meaningful features [32].

In addition to evaluating the aligner’s accuracy, we investigated and compared the time required to extract related concepts from unlabeled input images across the entire test set when using the DNN model’s representations and the trained aligner, versus directly using CLIP. We focus on the total execution time for concept extraction across the entire test set, because this step (the second step in Section III-A) directly influences the overall efficiency of an input selection strategy that leverages the CBD score. Measuring the cost of this step enables us to assess how the time required for concept extraction influences both the efficiency of CBD computation and the overall effectiveness of CBD-based input selection

TABLE II: Information on the trained linear aligners, including each DNN’s representation size, CLIP’s embedding size, coefficient of determination (R^2), and the time (in seconds) required to extract the related concepts for the entire test set using CLIP directly and using the trained aligner with the DNN models

input set	DNN’s representation size	CLIP’s embedding size	R^2	DNN’s execution time	CLIP’s execution time
Cifar-10	512	512	0.83	3.5 s	4 s
ImageNet	2048	512	0.72	105 s	36 s

when using either the DNN model representations mapped with the aligner or CLIP directly.

As reported in Table II, for smaller networks like ResNet18, the required time to execute the DNN model to extract test input representation and then apply the trained aligner (with negligible execution time) to map those representations to CLIP’s embedding space is less than that of running CLIP itself for concept extraction. In contrast, for deeper networks like ResNet101, running the DNN on all inputs takes longer than running CLIP directly. These results may suggest that for such DNNs, it is more efficient to extract concepts directly using CLIP. However, it is important to emphasize that, in most input selection strategies, including our CBD-based selection approach, diversity is not the sole guiding metric [4], [6].

Input selection approaches usually leverage diversity scores together with other metrics, such as the model’s uncertainty in predicting an input [6], which inherently requires evaluating all unlabeled inputs against the DNN model. In such scenarios, an input can be processed by the DNN model to simultaneously obtain its representation and estimate the model’s uncertainty, whereas running CLIP would introduce an extra cost. Therefore, since our proposed input selection approach leverages both the CBD and uncertainty metrics, we train and use a linear aligner to avoid the additional overhead of CLIP execution. Nevertheless, when only the CBD score is required, it can be calculated directly using concepts extracted from CLIP. The high accuracy of our trained aligners ensures that the resulting CBD scores closely approximate those computed directly using CLIP.

D. Data Availability

The replication package for our studies will be shared upon the paper’s acceptance [25].

V. RESULTS

In this section, we present the results related to our research questions and discuss their practical implications.

A. RQ1: Effectiveness of the CBD score

To address this research question, we require a large number of input subsets with varying diversity. To create these subsets, we followed a controlled process similar to that adopted in [7], as described in Section IV-A, to systematically create input subsets with increasing actual diversity. It is important to note that for input sets with a large number of output classes,

TABLE III: Spearman correlation coefficients computed between concept-based diversity and GD

Input set	Input subset size				
	$b=1\%$	$b=3\%$	$b=5\%$	$b=7\%$	$b=10\%$
Cifar-10	0.90	0.95	0.95	0.95	0.91
ImageNet	0.92	0.92	0.93	0.94	0.96

such as ImageNet, which contains 1000 classes, we need to start the controlled subset selection from more than one class, even for the smallest selection budget (e.g., 1% of the test set corresponds to 500 inputs). This is because each class has a relatively small number of inputs (only 50 per class in ImageNet).

Therefore, we start by randomly selecting a limited number of classes (e.g., 10) and randomly sampling a subset of size b from them. While keeping the subset size fixed at b , we gradually increase the number of classes represented in the subset by replacing some inputs with new ones from a new class. As the number of covered classes grows, the actual diversity of the subset increases, even though its size remains constant. At the initial stage and after each increment, we measured the CBD and GD scores for each subset, as described in Section IV-A. Subsequently, we conducted a correlation analysis between the computed CBD score and the GD score of these input subsets. Specifically, we measured the correlation between CBD and GD using the nonparametric Spearman’s rank correlation coefficient across all subsets, since we cannot assume linearity. Furthermore, we repeated this analysis for input subsets of different sizes corresponding to 1%, 3%, 5%, 7%, and 10% of the original test set for each subject. The correlation results for all subjects and subset sizes are reported in Table III. These results demonstrate that our proposed CBD score has a strong correlation with the GD score, with a minimum Spearman coefficient of 0.90 across all subjects and subset sizes. This finding validates the effectiveness of the CBD metric in accurately measuring the actual diversity of an input subset.

Answer to RQ1: The CBD scores have a strong Spearman correlation with GD scores, an established diversity metric known to align closely with the actual diversity of an input subset. This strong correlation indicates that CBD can effectively guide input selection to improve the DNN model.

B. RQ2: Efficiency of the CBD score calculation

To answer this research question, we evaluate the computation time required to calculate CBD scores and compare it with the time required to calculate GD scores. We report the computation time for input subsets used in the correlation analysis experiment designed to answer the previous question. It is important to note that when measuring the calculation time for the concept-based diversity, we consider only the time required to perform the second step of its calculation. As explained in Section III-A, the initialization step, building

TABLE IV: Average diversity calculation time (milliseconds) for a single subset of different sizes using CBD and GD

Input set	Metric	Input subset size				
		$b=1\%$	$b=3\%$	$b=5\%$	$b=7\%$	$b=10\%$
Cifar-10	CBD	0.3	0.7	1.1	1.53	2.2
	GD	1.8	2.5	3.1	5.3	14.6
ImageNet	CBD	1.4	4.2	6.9	9.4	12.5
	GD	3.7	27.4	96.7	203.3	437.9

a linear aligner and creating the RCS, is performed only once for each input set and DNN model, whereas the second step is performed multiple times for all the subsets. Therefore, the cost of the second step reflects the practical computational cost of deploying the CBD metric during input selection. The results are reported in Table IV.

The reported results confirm the computational efficiency of the proposed CBD metric. Across all input sets and subset sizes, calculating CBD scores consistently requires significantly less time than calculating GD scores. It is important to note that the reported computation times correspond to the average time required to calculate the diversity score for a single subset, whereas in most input selection strategies, such as search-based or adaptive random testing, diversity scores must be calculated repeatedly across many candidate subsets. Consequently, the execution time difference between CBD and GD becomes practically significant in the context of input selection.

As expected, the computation time for both metrics increases with the size of the input subset. However, this increase is substantially greater for the GD metric than for CBD. These results highlight the substantial computational advantage of CBD, especially for larger input sets such as ImageNet. In such scenarios, not only is the subset selection budget larger, but also the selection process involves computing the diversity of a significantly greater number of candidate subsets, further amplifying the computational cost of input selection. While both metrics are affected by both the input set size and the DNN model depth and complexity, CBD exhibits far superior scalability, maintaining its efficiency across different DNN architectures and input set sizes.

These findings, together with those from the first research question, demonstrate that CBD provides a level of diversity measurement effectiveness comparable to the GD metric at a fraction of its computational cost, making it a highly practical metric for large-scale input selection scenarios.

Answer to RQ2: The results demonstrate that CBD is significantly more computationally efficient than the GD metric. Across all input sets and subset sizes, CBD requires roughly 2.5 to 36 times less computation time while achieving comparable diversity measurement effectiveness. This finding confirms CBD as a practical and scalable diversity metric for large-scale DNN input selection.

TABLE V: Average accuracy improvement percentages achieved by fine-tuning the DNN model with input subsets selected by the CBD-based approach and each baseline (five runs)

Input set	Selection size	CBD-based selection	Baselines				
			Margin	DATIS	RTS	DeepGD	SETS
Cifar-10	$b=3\%$	67.48%	58.12%	32.72%	64.68%	66.17%	36.06%
	$b=5\%$	73.23%	72.63%	51.94%	61.11%	54.98%	45.12%
	$b=7\%$	72.61%	53.76%	56.98%	66.4%	45.7%	49.85%
	$b=10\%$	86.48%	50.48%	35.45%	69.36%	55.24%	44.24%
	$b=15\%$	82.06%	50.42%	34.87%	55.8%	54.6%	50.49%
	$b=20\%$	92.68%	47.15%	28.69%	34.19%	67.98%	54.32%
ImageNet	$b=5\%$	22.66%	7.29%	10.91%	19.68%	7.79%	9.37%
	$b=7\%$	32.37%	11.56%	26.68%	23.04%	15.10%	24.26%
	$b=10\%$	33.27%	20.12%	28.16%	11.63%	19.66%	30.72%
	$b=15\%$	41.81%	16.80%	32.62%	18.84%	32.89%	39.52%
	$b=20\%$	62.20%	24.64%	48.39%	38.84%	34.35%	37.53%

C. RQ3: Effectiveness of CBD-based input selection in guiding DNN model accuracy improvement

To address this research question, we investigated the improvement in DNN model accuracy achieved by fine-tuning with input subsets selected by our CBD-based approach. We compared it with all selection baselines outlined in Section II-A. To ensure a fair comparison, we adopted the same configurations and parameter settings provided in the original implementation of each baseline. However, to be able to apply DeepGD [6] on ImageNet, we reduced the number of generations in the NSGA-II algorithm to 10, due to the prohibitive computational cost of running NSGA-II with its default 300 generations on such a large input set.

To perform our experiments, we first divided each subject's original test sets in Table I into two equal candidate and validation sets. For subjects with the ImageNet input set, we used a 70% candidate and 30% validation split, since ImageNet contains a large number of classes, requiring larger input subsets to effectively fine-tune deeper, more complex models such as ResNet-101. Subsequently, we perform our experiment by selecting inputs from the candidate set and measuring the accuracy of both the original and fine-tuned models on unseen inputs in the validation set.

We applied our CBD-based selection approach, along with all selection baselines outlined in Section II-A, to select input subsets with different sizes from the candidate set across all subjects. Then, we used each subset chosen to fine-tune the subject DNN models by training them for a few more epochs. Consequently, the absolute performance improvements provided by each approach can be calculated as the difference between the fine-tuned model's accuracy and the original model's accuracy on the unseen validation set. However, the absolute accuracy difference does not account for the maximum improvement achievable for a given subject model. To address this, we consider the maximum potential improvement achievable by fine-tuning the model on the entire candidate set. This value represents the upper bound on accuracy improvement, i.e., the accuracy gain achievable if all candidate inputs were labeled and used during fine-tuning.

Therefore, we calculate the accuracy improvement percentages for each subject and selection budget as follows:

$$\text{Imp} = \left(\frac{\text{Acc}_{\text{fine-tuned}} - \text{Acc}_{\text{original}}}{\text{Acc}_{\text{max}} - \text{Acc}_{\text{original}}} \right) \times 100 \quad (3)$$

where $\text{Acc}_{\text{fine-tuned}}$, $\text{Acc}_{\text{original}}$, and Acc_{max} represent the accuracy of the fine-tuned model, original model, and the maximum accuracy of the model fine-tuned by the entire candidate set, respectively, all evaluated on the unseen validation set. Compared to calculating absolute improvements, this normalization formula enables a fair comparison across budgets and subjects.

To eliminate the impact of the inherent stochasticity of the fine-tuning process, we repeated fine-tuning for each selected subset five times with different random seeds and report the average accuracy improvement across runs. Table V presents the average accuracy improvement percentages achieved by the CBD-based approach and all selection baselines for all subjects and selection budgets. In this table, very small selection budgets in which subsets were selected by none of the investigated selection approaches were omitted, as these did not significantly improve the DNN model. For instance, for Cifar-10 and ResNet-18, none of the subsets selected with a budget $b=1\%$ could improve the model, whereas for ImageNet with the deeper, more complex ResNet-110, subsets selected with budgets $b=1\%$ and 3% are removed. This is because these subsets are too small to update the weights of a deep model, and thus, are unable to significantly improve its accuracy.

The highest achieved accuracy improvement for each subject and selection budget in Table V is highlighted in bold. The results demonstrate that the CBD-based approach consistently outperforms all baselines across subjects and selection budgets. To evaluate the statistical significance of these improvement differences, we conducted Wilcoxon signed-rank tests comparing the improvements from the CBD-based approach with each baseline at a significance level of $\alpha = 0.05$. Results show that all p-values are below 0.05, confirming that the improvements achieved by the CBD-based approach are statistically significant. Moreover, the CBD-based approach

TABLE VI: Selection time (in seconds) of the proposed CBD-based selection and each baseline

Input set	Selection size	CBD-based selection	Baselines				
			Margin	DATIS	RTS	DeepGD	SETS
Cifar-10	$b=3\%$	2	2	5	72	959	0.3
	$b=5\%$	2	2	5	72	1,341	0.5
	$b=7\%$	2	2	5	72	1,966	1
	$b=10\%$	2	2	5	72	3,476	2
	$b=15\%$	2	2	5	72	5,293	5
	$b=20\%$	3	2	5	72	9,067	12
ImageNet	$b=3\%$	71	70	970	73,080	2,644	67
	$b=5\%$	73	70	970	73,080	4,960	86
	$b=7\%$	76	70	970	73,080	8,292	254
	$b=10\%$	85	70	970	73,080	25,984	826
	$b=15\%$	111	70	970	73,080	89,174	2796
	$b=20\%$	154	70	970	73,080	233,744	7091

achieves practically significant average accuracy improvements of 79% on CIFAR-10 and 38% on ImageNet across all selection budgets. These results correspond to an average gain of approximately 13.9 percentage points on CIFAR-10 and 6.7 percentage points on ImageNet relative to the second-best-performing selection baselines across all selection budgets.

It is important to note that across all the investigated selection approaches in our study, increasing the selection budget does not necessarily lead to a monotonic increase in the percentage improvement in accuracy. Since these results present the average accuracy improvement percentages across five fine-tuning runs, such fluctuations are unlikely to be due to stochastic effects. Instead, they are primarily attributed to the catastrophic forgetting phenomenon [33]. As defined by Toneva *et al.* [33], a forgetting event occurs when an individual training example transitions from being correctly classified to incorrectly classified over the course of learning, even without a distributional shift. This dynamic results in non-monotonic performance trends as additional inputs or training iterations are introduced, since newly included or reweighted inputs can both reinforce and interfere with previously learned representations. In our experiments, we observed a similar behavior across all selection approaches, including our proposed CBD-based selection, suggesting that model updates, even on diverse subsets, repeatedly induce localized forgetting and relearning dynamics. Nonetheless, the CBD-based selection consistently outperforms the baselines across all selection budgets, demonstrating its strong generalizability.

Answer to RQ3: The CBD-based selection approach consistently outperforms all baselines in guiding input selection for improving the DNN model across all subjects and selection budgets. Furthermore, CBD-based selection provides statistically significant accuracy improvements, achieving average accuracy increases of 79% and 38% across all budget sizes for Cifar-10 and ImageNet, respectively.

D. RQ4: Efficiency of CBD-based input selection

To answer this research question, we empirically evaluate the computational efficiency of the proposed CBD-based selection approach by comparing its selection time with that of all baselines. Specifically, we measure the time required by each approach to select unlabeled input subsets of varying sizes from each subject’s candidate set. Table VI provides the selection time (in seconds) for our CBD-based approach and each baseline when selecting subsets corresponding to 3%, 5%, 7%, 10%, 15%, and 20% of the candidate set.

As shown in Table VI, the selection time for input prioritization approaches, including uncertainty metrics such as Margin and DATIS, as well as RTS, remains constant across different selection budgets. This is because these approaches calculate a priority score for all unlabeled candidate inputs once and then rank them, producing an ordered list of inputs. Then, a subset can be selected from the top of the ordered list based on the required number of inputs, within the selection budget. As a result, their selection time is independent of the selection budget and depends solely on the time needed to rank all inputs in the candidate set.

In contrast, for selection approaches such as the proposed CBD-based selection and DeepGD, the selection time varies across different selection budgets. It is important to note that, while the proposed CBD-based approach first ranks all candidate inputs by their uncertainty score, as with prioritization approaches, it also iteratively calculates the CBD score for multiple candidate subsets until the specified selection budget is reached. Consequently, the total selection time of the CBD-based approach includes both the initial ranking time and the subsequent diversity calculation time.

It is important to note that to ensure a fair and consistent comparison, we report execution times in this table on a server equipped with an Intel® Xeon® Gold 6234 CPU (16 cores, 3.30 GHz), 192 GB of RAM, and an Nvidia Quadro RTX 6000 GPU with 24 GB of memory.

The results in Table VI demonstrate that the CBD-based selection is highly efficient, requiring selection time close to that of simple output-probability-based uncertainty metrics,

such as Margin, even on larger input sets. These selection times are significantly lower than those of the diversity-based and other hybrid baselines, such as DeepGD and RTS. For instance, selecting a subset with $b = 20\%$ from ImageNet takes roughly 154 seconds using the CBD-based approach, whereas DeepGD and RTS require 233,744 and 73,080 Seconds, respectively. It is important to note that the reported selection time for DeepGD on the CIFAR-10 input set is based on the default NSGA-II configuration of 300 generations. In contrast, for the ImageNet input set, this parameter was reduced to 10 generations, as running NSGA-II with the default 300 generations would require more than 80 days of computation, rendering it practically infeasible.

The results in Table VI further indicate that hybrid baselines are computationally expensive, primarily due to the high cost of diversity calculations. Although SETS [34] is the least expensive among the hybrid baselines, it still requires substantially higher selection time than the proposed CBD-based selection and the neighbor-aware uncertainty-based baseline, DATIS [16]. In contrast, the CBD-based selection remains highly efficient, even on larger input sets like ImageNet, requiring significantly less time than DATIS while retaining the benefits of diversity-based selection.

While prioritization-based selection approaches, such as Margin and DATIS, as well as RTS, require the same time to select subsets of varying sizes (for the reasons discussed above), the selection time for all other approaches increases with the selection budget. However, this increase is substantially smaller for the CBD-based approach than for SETS and DeepGD. For instance, selecting a subset with $b=10\%$ from ImageNet requires only about 14 more seconds than with $b=3\%$ for the CBD-based approach, whereas DeepGD requires about 23,340 more seconds (about 10 times as much). This further confirms the scalability and practical efficiency of the CBD-based selection approach.

Answer to RQ4: The CBD-based selection approach remains highly efficient with selection times close to simple uncertainty-based selections such as Margin. In contrast, diversity-based and hybrid baselines, such as RTS and DeepGD, require significantly more selection time, particularly on larger input sets such as ImageNet. These results further highlight not only the practicality and computational advantage of the CBD-based approach but also its scalability, particularly for larger input sets.

E. Threats to Validity

In this section, we discuss the different potential threats to the validity of our study and describe how we mitigated them.

Construct threats to validity. A potential threat relates to the implementation of input selection baselines. To reduce the risk of implementation bias, we used the original implementations provided by the respective authors. Another threat concerns the accuracy improvement metric we used to evaluate the proposed approach. To mitigate this threat and provide a

fair comparison between CBD-based selection and baselines across all subjects and selection budgets, we account for the maximum potential improvement achievable by fine-tuning the model on the entire candidate set in our accuracy improvement measurements.

Internal threats to validity. One internal threat to validity concerns the selection of parameters and experimental configurations for both the baseline and the proposed approach. To mitigate this concern, we used the same settings provided in the original implementation of each baseline. We note, however, that applying DeepGD [6] to the ImageNet input set required a practical adjustment. Due to the prohibitive computational cost of running NSGA-II with its default 300 generations on such a large input set, we reduced the number of generations to 10. The CBD-based selection approach relies on the parameter m , which controls the number of concepts extracted from each image input for calculating the CBD score. As we described in Section IV, we followed a simple manual procedure to determine an appropriate value for this parameter in our experiments. While the current results with $m = 10$ are encouraging, optimizing this parameter may further improve CBD-based selection performance. Another internal threat arises from the inherent randomness involved in fine-tuning DNN models using the selected inputs. We addressed this issue by repeating the fine-tuning process five times with different random seeds for each combination of selection budget, input set, and model, thereby reducing the impact of stochastic variations on our results.

External threats to validity. To address potential concerns about the generalizability of the CBD-based selection approach, we conducted experiments across multiple subjects, covering diverse combinations of DNN models with varying internal architectures and input sets comprising different image types. In particular, we included large input sets such as ImageNet to evaluate the scalability and practical applicability of the proposed approach. Additionally, the CBD-based selection approach was evaluated across a wide range of input selection budgets to assess its robustness under varying resource constraints. Across all combinations of input sets, model architectures, and selection budgets, the results consistently demonstrated substantial improvements in model accuracy, indicating strong generalizability across diverse experimental settings.

VI. RELATED WORK

In this section, we first review existing work on input selection approaches for image DNN models. We then briefly summarize prior work that leverages VLMs to analyze and evaluate image classification DNNs.

A. DNN input selection

In recent years, several approaches to input selection have been proposed for DNN models. However, many of them are ineffective at improving the DNN model and are consistently outperformed by more recent approaches. For instance, several early contributions in input selection, such as NC [12], [13], Cross Entropy-based Sampling (CES) [35], and SA [11], have

been extensively studied in recent work. NC metrics assess inputs based on the extent to which neuron activation ranges are exercised. In contrast, SA metrics quantify how surprising an unlabeled input is with respect to the DNN’s training input distribution. CES, in contrast, prioritizes inputs based on the representations learned by the DNN under test, where each input is characterized by the probability distribution of neuron outputs in the last hidden layer, and selection is guided by minimizing cross-entropy. All of these approaches, NC, AS, and CES, have been consistently outperformed by more recent input selection approaches, including several baselines in our experiments, such as RTS [8] and DATIS [16].

Uncertainty metrics are one of the most efficient selection approaches proposed for DNNs [4], [15], [14], [16]. These metrics measure the DNN model’s confidence in predicting an input and are used to prioritize selecting inputs for which the model is less confident, i.e., those it is more likely to mispredict. Simple uncertainty metrics such as DeepGini [14], Vanilla-Softmax [15], and Margin [4] are calculated solely based on the model’s output probability vector [4]. Although DeepGini and Vanilla-Softmax have been widely used as baselines in prior work, including some of the baselines in our experiments, recent studies have consistently shown that they are outperformed by more advanced uncertainty-based and hybrid selection approaches [6], [10], [8], [16]. However, SOTA uncertainty metrics such as DATIS [16] combine the model’s output probability for a given input with information from its nearest neighbors to calculate the input’s uncertainty score. Consequently, we also include Margin and DATIS as baselines. However, our proposed CBD-based selection approach outperformed both Margin and DATIS across all subjects and selection sizes.

Diversity-based approaches are also among the well-studied and effective selection approaches for DNNs. Gao *et al.* introduced ATS [10], which iteratively selects inputs that have less similarity with the currently selected subset. This incremental selection strategy requires calculating the dissimilarity between each remaining input and the currently selected subset, making it one of the most computationally intensive selection approaches [4]. Moreover, ATS has been consistently outperformed by three baselines in our experiments: DeepGD [6], RTS [8], and DATIS [16], both for fault detection and for improving DNN models. Diversity metrics for image inputs, including Normalized Compression Distance, Standard Deviation, and GD, have been comprehensively investigated by Aghababaeyan *et al.* [7]. Their empirical results demonstrate that GD is the most effective metric for capturing the true diversity of an input set and, consequently, for guiding input selection to test and improve DNN models. However, to enhance the input selection performance, they combined the GD metric with DeepGini, a simple uncertainty metric, and proposed DeepGD [6], a hybrid multi-objective selection approach.

In recent years, hybrid input selection strategies have received increasing attention, leading to the development of several effective approaches. These approaches primarily combine diversity and uncertainty metrics, leveraging their complementary strengths to select input subsets that are both diverse and

highly effective at detecting faults, while also improving DNN performance through fine-tuning. Among these SOTA hybrid approaches, RTS [8], DeepGD [6], and SETS [34] are included in our study as representative baselines.

A key limitation of these hybrid approaches lies in their computational cost. Calculating diversity for a large number of candidate subsets, combined with running multi-objective selection algorithms such as NSGA-II, can be highly resource-intensive. As our results demonstrate, while DeepGD and RTS are among the most effective approaches, they are computationally expensive and may even be impractical in extensive selection scenarios. SETS [34], proposed by Wang *et al.*, attempts to mitigate this issue by incorporating a massive input reduction phase along with a highly restrictive selection process. Our results show that SETS substantially reduces the number of diversity calculations, making it less computationally expensive than RTS and DeepGD. However, the proposed CBD-based selection is highly efficient, requiring significantly less selection time than SETS. Moreover, this reduction and restrictive selection of SETS also limit its effectiveness compared to the proposed CBD-based selection approach.

In contrast, our proposed CBD-based selection approach avoids discarding potentially valuable inputs and imposes no restrictive selection constraints. Instead, it significantly reduces the time required to compute diversity for each candidate subset by leveraging VLMs. As a result, the CBD-based approach achieves both high efficiency and high effectiveness, consistently outperforming all baselines, including existing hybrid methods, in improving DNN models.

In addition to uncertainty- and diversity-based input selection, some approaches move beyond purely heuristic metrics by exploiting structural or theoretical properties of DNN models. Multiple-Boundary Clustering and Prioritization (MCP) [27] clusters unlabeled inputs that lie near decision boundaries by leveraging the model’s output probability distributions. It then selects inputs evenly from these boundary-specific clusters, ensuring balanced coverage of decision regions while avoiding redundant selection from densely populated areas. In contrast, CertPri adopts a different perspective by introducing a certifiable upper bound on the retraining gain of each unlabeled input. This bound is derived from a theoretical analysis of the expected reduction in training loss when incorporating a specific input during retraining. Nevertheless, both MCP and CertPri are outperformed by more recent approaches [16], [8], [6], including some of our baselines such as DATIS, RTS, and DeepGD.

Other input selection approaches, such as Mutation testing [36], [37] or other search-based selections [38] based on the NSGA-II algorithm, have also been proposed for DNN models. However, their huge computation cost limits their application in extensive selection scenarios. Consequently, we exclude those approaches from our study, given that performance and scalability are the main objectives.

B. DNN model analysis and testing using VLMs

Since the introduction of VLMs, they have been leveraged to analyze and improve DNN models. In a recent study, Hu

et al. leveraged VLMs such as CLIP for runtime analysis of image classification DNN models and for localizing faults in their networks. They introduce semantic heatmaps to represent the frequency with which a specific concept is observed in correctly and incorrectly classified inputs from the model’s training set. They then use these heatmaps to evaluate unlabeled inputs during runtime. Based on the similarity of a given input to each heatmap, they can predict whether the model will misclassify or correctly classify the input and, finally, estimate the model’s accuracy. Furthermore, by performing zero-shot classification with a VLM, they identify whether misclassifications are due to faults in the DNN model’s encoder or classification head. While the objectives of this approach differ from our goal, they share the basic idea of using VLMs to calculate the similarity between an image and a natural-language concept. However, one of the main limitations of this approach is that, to create concept heatmaps, they manually define a small, fixed set of concepts for each input class. Consequently, building heatmaps for input sets with a large number of input classes, such as ImageNet with 1000 classes, is not feasible.

VII. CONCLUSION

In this paper, we introduce Concept-based Diversity (CBD), a new metric that effectively and efficiently measures the diversity of image input sets using Vision-Language Models (VLMs). Our evaluations show that the CBD score effectively captures the true diversity of images in an input set. More importantly, the CBD calculation is highly efficient, making it a scalable metric for repetitive, extensive input selection scenarios. Leveraging this metric, we propose a hybrid CBD-based input selection approach for DNN models that combines the model’s uncertainty with the diversity of the input set to select a small yet informative and representative subset of inputs for labeling and to improve the model through fine-tuning. We conducted an extensive empirical study to evaluate our CBD-based selection approach, comparing it against five highly effective SOTA baselines. The results show that the proposed approach consistently outperforms all baselines in terms of model accuracy improvement while being among the most efficient approaches, requiring calculation times close to those of simple uncertainty metrics such as Margin.

ACKNOWLEDGEMENTS

This work was supported by the Canada Research Chair and Discovery Grant programs of the Natural Sciences and Engineering Research Council of Canada (NSERC) and the Research Ireland grant 13/RC/2094-2.

REFERENCES

- [1] J. Chai, H. Zeng, A. Li, and E. W. Ngai, “Deep learning in computer vision: A critical review of emerging techniques and application scenarios,” *Machine Learning with Applications*, vol. 6, p. 100134, 2021.
- [2] Y. Yang, X. Xia, D. Lo, and J. Grundy, “A survey on deep learning for software engineering,” *ACM Computing Surveys (CSUR)*, vol. 54, no. 10s, pp. 1–73, 2022.
- [3] A. A. Shahkoo and A. A. Abin, “Autonomous tissue manipulation via surgical robot using deep reinforcement learning and evolutionary algorithm,” *IEEE Transactions on Medical Robotics and Bionics*, vol. 5, no. 1, pp. 30–41, 2023.
- [4] Q. Hu, Y. Guo, X. Xie, M. Cordy, L. Ma, M. Papadakis, and Y. Le Traon, “Test optimization in dnn testing: a survey,” *ACM Transactions on Software Engineering and Methodology*, vol. 33, no. 4, pp. 1–42, 2024.
- [5] A. Radford, J. W. Kim, C. Hallacy, A. Ramesh, G. Goh, S. Agarwal, G. Sastry, A. Askell, P. Mishkin, J. Clark *et al.*, “Learning transferable visual models from natural language supervision,” in *International conference on machine learning*. PMLR, 2021, pp. 8748–8763.
- [6] Z. Aghababaeyan, M. Abdellatif, M. Dadkhah, and L. Briand, “Deepgd: A multi-objective black-box test selection approach for deep neural networks,” *ACM Transactions on Software Engineering and Methodology*, vol. 33, no. 6, pp. 1–29, 2024.
- [7] Z. Aghababaeyan, M. Abdellatif, L. Briand, M. Bagherzadeh *et al.*, “Black-box testing of deep neural networks through test case diversity,” *IEEE Transactions on Software Engineering*, vol. 49, no. 5, pp. 3182–3204, 2023.
- [8] W. Sun, M. Yan, Z. Liu, and D. Lo, “Robust test selection for deep neural networks,” *IEEE Transactions on Software Engineering*, vol. 49, no. 12, pp. 5250–5278, 2023.
- [9] O. Russakovsky, J. Deng, H. Su, J. Krause, S. Satheesh, S. Ma, Z. Huang, A. Karpathy, A. Khosla, M. Bernstein, A. C. Berg, and L. Fei-Fei, “ImageNet Large Scale Visual Recognition Challenge,” *International Journal of Computer Vision (IJCV)*, vol. 115, no. 3, pp. 211–252, 2015.
- [10] X. Gao, Y. Feng, Y. Yin, Z. Liu, Z. Chen, and B. Xu, “Adaptive test selection for deep neural networks,” in *Proceedings of the 44th International Conference on Software Engineering*, 2022, pp. 73–85.
- [11] J. Kim, R. Feldt, and S. Yoo, “Guiding deep learning system testing using surprise adequacy,” in *2019 IEEE/ACM 41st International Conference on Software Engineering (ICSE)*. IEEE, 2019, pp. 1039–1049.
- [12] K. Pei, Y. Cao, J. Yang, and S. Jana, “Deepxplore: Automated whitebox testing of deep learning systems,” in *proceedings of the 26th Symposium on Operating Systems Principles*, 2017, pp. 1–18.
- [13] L. Ma, F. Juefei-Xu, F. Zhang, J. Sun, M. Xue, B. Li, C. Chen, T. Su, L. Li, Y. Liu, J. Zhao, and Y. Wang, “Deepgauge: Multi-granularity testing criteria for deep learning systems,” *2018 33rd IEEE/ACM International Conference on Automated Software Engineering (ASE)*, pp. 120–131, 2018.
- [14] Y. Feng, Q. Shi, X. Gao, J. Wan, C. Fang, and Z. Chen, “Deepgini: prioritizing massive tests to enhance the robustness of deep neural networks,” in *Proceedings of the 29th ACM SIGSOFT International Symposium on Software Testing and Analysis*, 2020, pp. 177–188.
- [15] M. Weiss and P. Tonella, “Simple techniques work surprisingly well for neural network test prioritization and active learning,” in *Proceedings of the 31th ACM SIGSOFT International Symposium on Software Testing and Analysis*, 2022.
- [16] Z. Li, Z. Xu, R. Ji, M. Pan, T. Zhang, L. Wang, and X. Li, “Distance-aware test input selection for deep neural networks,” in *Proceedings of the 33rd ACM SIGSOFT International Symposium on Software Testing and Analysis*, 2024, pp. 248–260.
- [17] S. Bao, C. Sha, B. Chen, X. Peng, and W. Zhao, “In defense of simple techniques for neural network test case selection,” in *Proceedings of the 32nd ACM SIGSOFT International Symposium on Software Testing and Analysis*, 2023, pp. 501–513.
- [18] A. Abbasishakoo, M. Dadkhah, L. Briand, and D. Lin, “Metasel: A test selection approach for fine-tuned dnn models,” *IEEE Transactions on Software Engineering*, 2025.
- [19] Q. Hu, Y. Guo, X. Xie, M. Cordy, W. Ma, M. Papadakis, and Y. L. Traon, “Evaluating the robustness of test selection methods for deep neural networks,” *arXiv preprint arXiv:2308.01314*, 2023.
- [20] R. Speer, J. Chin, and C. Havasi, “Conceptnet 5.5: An open multilingual graph of general knowledge,” in *Proceedings of the AAAI conference on artificial intelligence*, vol. 31, no. 1, 2017.
- [21] M. Moayeri, K. Rezaei, M. Sanjabi, and S. Feizi, “Text-to-concept (and back) via cross-model alignment,” in *International Conference on Machine Learning*. PMLR, 2023, pp. 25 037–25 060.
- [22] G. A. Miller, “Wordnet: a lexical database for english,” *Communications of the ACM*, vol. 38, no. 11, pp. 39–41, 1995.
- [23] R. Krishna, Y. Zhu, O. Groth, J. Johnson, K. Hata, J. Kravitz, S. Chen, Y. Kalantidis, L.-J. Li, D. A. Shamma *et al.*, “Visual genome: Connecting language and vision using crowdsourced dense image annotations,” *International journal of computer vision*, vol. 123, no. 1, pp. 32–73, 2017.
- [24] A. Kuznetsova, H. Rom, N. Alldrin, J. Uijlings, I. Krasin, J. Pont-Tuset, S. Kamali, S. Popov, M. Malloci, A. Kolesnikov *et al.*, “The open images dataset v4: Unified image classification, object detection, and visual relationship detection at scale,” *International journal of computer vision*, vol. 128, no. 7, pp. 1956–1981, 2020.

- [25] The link to these artifacts will be made publicly available upon acceptance of this paper.
- [26] K. Alex, N. Vinod, and H. Geoffrey. The cifar-10 dataset. [Online]. Available: <https://www.cs.toronto.edu/~kriz/cifar.html>
- [27] W. Shen, Y. Li, L. Chen, Y. Han, Y. Zhou, and B. Xu, "Multiple-boundary clustering and prioritization to promote neural network retraining," in *Proceedings of the 35th IEEE/ACM International Conference on Automated Software Engineering*, 2020, pp. 410–422.
- [28] A. Abbasishahkoo, M. Dadkhah, L. Briand, and D. Lin, "Teasma: A practical methodology for test adequacy assessment of deep neural networks," *IEEE Transactions on Software Engineering*, 2024.
- [29] Q. Hu, Y. Guo, M. Cordy, X. Xie, L. Ma, M. Papadakis, and Y. Le Traon, "An empirical study on data distribution-aware test selection for deep learning enhancement," *ACM Transactions on Software Engineering and Methodology (TOSEM)*, vol. 31, no. 4, pp. 1–30, 2022.
- [30] D. Berend, X. Xie, L. Ma, L. Zhou, Y. Liu, C. Xu, and J. Zhao, "Cats are not fish: Deep learning testing calls for out-of-distribution awareness," in *Proceedings of the 35th IEEE/ACM international conference on automated software engineering*, 2020, pp. 1041–1052.
- [31] K. He, X. Zhang, S. Ren, and J. Sun, "Deep residual learning for image recognition," in *Proceedings of the IEEE conference on computer vision and pattern recognition*, 2016, pp. 770–778.
- [32] Y. Bengio, A. Courville, and P. Vincent, "Representation learning: A review and new perspectives," *IEEE transactions on pattern analysis and machine intelligence*, vol. 35, no. 8, pp. 1798–1828, 2013.
- [33] M. Toneva, A. Sordoni, R. T. d. Combes, A. Trischler, Y. Bengio, and G. J. Gordon, "An empirical study of example forgetting during deep neural network learning," in *Proceedings of the International Conference on Learning Representations (ICLR)*, 2019.
- [34] J. Wang, H. Wu, P. Wang, X. Niu, and C. Nie, "Sets: A simple yet effective dnn test selection approach," *ACM Transactions on Software Engineering and Methodology*, 2025.
- [35] Z. Li, X. Ma, C. Xu, C. Cao, J. Xu, and J. Lü, "Boosting operational dnn testing efficiency through conditioning," in *Proceedings of the 2019 27th ACM Joint meeting on European software engineering conference and symposium on the foundations of software engineering*, 2019, pp. 499–509.
- [36] N. Humbatova, G. Jahangirova, and P. Tonella, "Deepcrime: mutation testing of deep learning systems based on real faults," in *Proceedings of the 30th ACM SIGSOFT International Symposium on Software Testing and Analysis*, 2021, pp. 67–78.
- [37] Q. Hu, L. Ma, X. Xie, B. Yu, Y. Liu, and J. Zhao, "Deepmutation++: A mutation testing framework for deep learning systems," in *2019 34th IEEE/ACM International Conference on Automated Software Engineering (ASE)*. IEEE, 2019, pp. 1158–1161.
- [38] Y. Hao, Z. Huang, H. Guo, and G. Shen, "Test input selection for deep neural network enhancement based on multiple-objective optimization," in *2023 IEEE International Conference on Software Analysis, Evolution and Reengineering (SANER)*. IEEE, 2023, pp. 534–545.